Separation of Chiral Mixtures in Real SMB Units: The FlexSMB-LSRE®

Pedro Sá Gomes, Miriam Zabkova, Michal Zabka, Mirjana Minceva, and Alírio. E. Rodrigues
Laboratory of Separation and Reaction Engineering, Associate Laboratory LSRE/LCM, Dept. of Chemical Engineering, Faculty of Engineering, University of Porto, Rua Dr. Roberto Frias, 4200-465 Porto, Portugal

DOI 10.1002/aic.11962
Published online August 4, 2009 in Wiley InterScience (www.interscience.wiley.com)

In this work, a procedure for the separation of a racemic mixture of guaifenesin onto a chiral stationary phase (Chiralpak AD), by means of Simulated Moving Bed (SMB) technology, is presented in four major steps: (1) search for the suitable stationary and mobile phases; (2) determination of sorption parameters and validation by frontal analysis; (3) modeling and design of the SMB unit; and (4) operation and demonstration. A major emphasis is given to the common deviations that "real" SMB units present when compared with the theoretical apparatus (due to tubing and equipment dead volumes, switching time asymmetries and delays, pumps flow rates variations). These deviations are analyzed before and after the design and construction of the FlexSMB-LSRE® unit, a new flexible unit, hereby presented. A detailed model that takes into account tubing and equipment dead volumes, as well as switching time asymmetries and delay, was used to study and compare different dead volumes design and compensating strategies. It is shown that all these approaches can be converged into a switching time compensating strategy. This approach served to predict the experimental operating conditions and run a classical SMB experiment, which afterwards was compared with the simulated profiles obtained for the FlexSMB-LSRE® unit. The result of the separation was guaifenesin enantiomers with purities above 98% and a productivity value of 23 $g_{enantiomer}/(dm^3\ CSP\ day)$. © 2009 American Institute of Chemical Engineers *AIChE J,* 56: 125–142, 2010

Keywords: simulated moving bed, SMB, true moving bed, TMB, guaifenesin separation, dead volumes, Chiralpak AD, modeling, switching time asymmetries

Introduction

In the past, most of the chiral drugs available on the market were presented in racemic forms. However, it was found that in the most of the cases each enantiomer possesses different biological activities, where one may be therapeutically nonactive or even antagonist.[1] Consequently, there has been an increasing demand to supply enantiomerically pure drugs for therapeutic purposes.[2] Although the desired enantiomer can be produced by specific synthesis procedures, such as enantioselective synthesis, the development these methods is usually costly and time consuming.[2,3] Regarding it, and to accelerate the marketing and reduce the expenses of new medicines, preparative chiral chromatography has been used to obtain sufficient product quantities for pharmacological and toxicological tests. In fact, one of the most useful resolution method applied in the area of chiral separation, besides chiral crystallization and enzymatic methods, has become chromatography, mainly based on chiral stationary phases (CSP).[1–3]

Traditionally, batch chromatography is considered a very expensive technique. Nevertheless, the continuous counter current apparatus have shown considerable advantages.[4] In fact, the use of continuous chromatographic counter current operation maximizes the mass transfer driving force, leading

Correspondence concerning this article should be addressed to A. E. Rodrigues arodrig@fe.up.pt

Current Address of Mirjana Minceva: Lehrstuhl für Thermische Verfahrenstechnik der Universität Erlangen-Nürnberg, Egerlandstr. 3, D-91058 Erlangen, Germany.

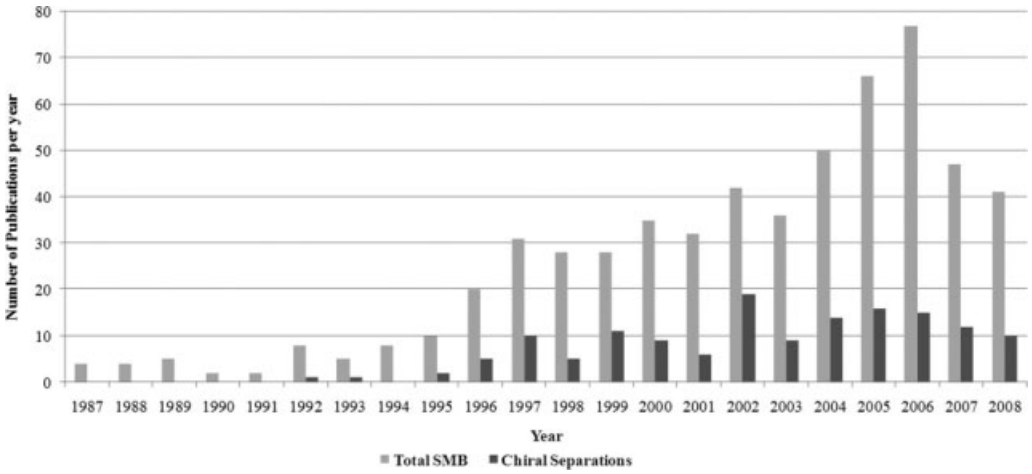

Figure 1. Publications regarding SMB applications over the past 20 years.[20]

to a better utilization of the adsorbent, which may have a rather low selectivity. In addition, the implementation of continuous techniques also reduces solvent consumption and increases productivity.[4] With the counter current operating mode it is possible to achieve high purity even if the resolution of the two peaks is not complete, contrary to batch chromatography where high resolution is a crucial parameter. However, the counter current flow of a solid phase inside of a given column and its recirculation presents several technical problems, namely: mechanical erosion of adsorbent (leading to particle size redistribution, capacity decline, channeling, pressure drop); equipment abrasion; difficulties in maintaining plug flow for a solid phase, which will clearly limit the implementation of such technologies. To avoid these problems, a sequence of fixed bed columns was conceived by Broughton and Gerhold,[5] where the solid phase does not move. The relative movement between both fluid and solid streams is created by switching all inlet and outlet fluid streams from time to time in the direction of the fluid flow and by this means simulating a contrary solid movement, the Simulated Moving Bed (SMB) technology, by opposition with the continuous counter current system or True Moving Bed (TMB).

Traditionally, SMB applications can be regarded as ''Old'' and ''New,'' associated with petrochemical and pharmaceutical/fine chemistry fields, respectively.[6] Among the first applications of this technology (back to 1960s) is the Parex® unit (UOP, Des Plaines-IL) for separation of *p*-xylene from mixtures with the C_8-isomers.[7] In the last decade, particularly in the area of drug development, the advent of SMB technology has provided a high throughput, high yield, solvent efficient, safe, and cost effective process option. Although being considered as a viable, practical, and a cost-effective liquid-phase adsorptive separation technique, the pharmaceutical and biomolecule separations community did not show considerable interest in SMB technology until the mid-1990s,[3,8–19] as it is shown by the number of publications concerning chiral separations, Figure 1.

In 1992, Daicel Chemical Industries (Japan) first published the resolution of optical isomers by means of SMB.[21] Since that time, a considerable number of articles, patents, and books related with the application of SMB to pharmaceutically important compounds have been published and approved by the Food and Drug Administration (FDA) for some Active Principle Ingredient (API) production. Several are the separations already running, associated with renowned products such as: Biltricide (Praziquantel) Cipralex/Lexapro (Escitalopram), Keppra (Levetiracetam), Modafinil/Provigil, Taxol (Paclitaxel), Xyzal (Levocetirizine), Zoloft (Sertraline), Zyrtec (Cetirizine), Celexa/Citrol/Cipram (Citalopram), Prozac (Fluoxetine hydrochloride), and insulin among others.[22]

This late interest in fine chemical separations led to the development of several SMB operation modes, such as the introduction of the asynchronous inlet/outlet ports shift as proposed by Novasep (Pompey, France)[23] with the Varicol® technique; the modulation of the feed flow rate proposed with the PowerFeed[24] technique and partial feed[25]; variable feed concentration with the Modicon mode of operation[26,27]; the Outlet Swing Stream-SMB operating mode[28]; and hybrid processes such as the M3C process,[29,30] or the Enriched Extract operation (EE-SMB),[31] in which a portion of the extract product is concentrated and then reinjected into the SMB at the same collection point, among others.

Nevertheless, the practical application of these so-called ''non-conventional'' SMB operating modes in the existing commercial SMB units is a challenging task. Generally, an SMB unit (industrial, pilot, or laboratory-scale) is limited to one or two modes of operation and to implement a new operating mode is necessary to contact the supplier, do adjustments, even to reformulate the entire unit if not to acquire a new one. Therefore, flexibility (at least at laboratory-scale) is seen as one of the more relevant qualities for this kind of equipment. This aspect was the main reason that led to the design and construction of a six columns unit at LSRE, the FlexSMB-LSRE®, hereby presented.

Commonly, the used modeling and simulation methodologies for SMB units do not account for pipe transfer lines and the surrounding equipment (valves, degassers, pumps). At industrial-scale SMB units, the relative volume of the connection lines is not that significant as in the pilot or lab-scale units. Nevertheless, it has been studied in detail and different techniques are applied to overcome the associated negative impacts on the SMB performances. For instance, the

UOP technique for flushing of the transfer lines before withdrawing the extract, applied in Parex process/(industrial scale SMB unit for *p*-xylene separation), was previously analyzed.[32]

In pilot or lab-scale SMB units, the relative volume associated with equipment and transfer lines is indeed an issue and therefore it has to be taken into account even before unit's design and construction, as well as during its operation. Usually this type of units are designed to account for it in its own operation mode, and thus compensating it,[33,34] or extended design methodologies are used to account for it during the design procedure.[35,36] Nevertheless, these are still proxies to the use of more detailed models and some differences are noted between the results obtained by means of the commonly used models and experimental results.

The objective of this work is then to detail a procedure for the separation of a racemic mixture by means of SMB technology, hereby classified into four major steps, namely:

(1) Search for the suitable stationary phase and mobile phases;

(2) Determination of sorption parameters and validation by Frontal Analysis (FA);

(3) Modeling, design, and construction of the SMB unit (determination of basic operating parameters);

(4) Operation and demonstration.

For this purpose, the separation of racemic guaifenesin mixture onto CSP Chiralpak AD was selected. This stationary phase is for the first time used in an SMB application for the separation of guaifenesin. The adsorption equilibrium of guaifenesin enantiomers was determined, and the appropriate adsorption isotherms were applied. The mathematical modeling and computer simulation of the experimentally obtained enantiomers concentration profiles was carried out in order to characterize and validate the system.

A detailed model accounting for equipment dead volumes, tubing connections, and switching time asymmetries and delay was used to model a lab-scale (FlexSMB-LSRE®) and a pilot-scale (Licosep 12-26) units and then used to compare dead volumes design and compensating strategies. The SMB-detailed model was utilized to obtain the separation region for the FlexSMB-LSRE® unit that served to corroborate a dead volumes switching time compensating strategy. This strategy was used to predict the experimental operating conditions and run a classical SMB experiment, which afterwards was compared with the simulated concentration profiles obtained for the FlexSMB-LSRE® unit.

Search for the Suitable Stationary and Mobile Phases

For an effective SMB process, as in batch chromatography, the selection of a suitable chiral stationary phase (CSP) and eluent/desorbent (mobile phase) are crucial. However, the requirements are slightly different from those valid for the batch chromatography. As mentioned before, some limiting aspects in batch chromatography, such as the peaks resolution, are not considered as substantial restrictions in the continuous counter current chromatography, in this case an SMB.

The effective enantioselectivity of the chromatographic system is proportional to the ratio of the enantioselectivity of the association processes in the stationary and mobile phases, therefore, a compromise between the separation factor, the capacity factor, and the solubility of solute must be also taken into account.

Chiral stationary phases

The enantiomeric resolution is only possible in chromatographic systems containing the appropriate chiral selector, which can be physically coated or bonded on the stationary phase carrier, in most of the cases silica spherical particles. Among a vast range of commercially available stationary phases only a few of CSPs are available for production scale,[3,37] such as: Pirkle type stationary phase, cellulose derivates, and amylose derivates. Recently, new and more versatile Daicel polysaccharide CSPs have been commercialized offering an enhanced separation potential. In the past years, the polysaccharide derivatives have started to be immobilized by covalent bonding on a silica matrix resulting in the development of brand new CSPs, which are more robust and compatible in terms of broad range of organic solvent systems.[1–3]

In this work, the stationary phase Chiralpak AD from Chiral Tech Europe was used and for the first time applied for this separation using SMB technology. This stationary phase was also successfully applied for the separation α-tetralol using a pilot-scale SMB unit (Licosep 12-26),[38] among other chiral compounds. The CPS Chiralpak AD is physically adsorbed on silica and thus limits the use of mobile phases to heptane, hexane, and alcohols, such as ethanol and methanol.

Selection of the mobile phase

The solubility of a given mixture in a mobile phase is an important aspect to be considered in order to increase the amount of racemate loaded in a single run. Other decisive factors for the mobile selection are: its compatibility with CSPs, total eluent consumption, possibility of recycling it, as well as, required duty of the final product purification. In SMB chromatography, it is seen as a good practice to keep the mobile phase composition as simple as possible, which means that the mobile phase should be a mixture of maximum of two different solvents, even if the separation of the enantiomers is only partial.

As a result, it should be given a major importance to this preceding step to the SMB design and consider the following points:

(1) Setting of the separation requirement (productivity, purity);

(2) Determination of solubility of the species in the mobile phase;

(3) Selectivity screening (involving different mobile phases and composition);

(4) Optimization of mobile phase/stationary phase combinations (retention time, elution order, temperature, simplicity, economical factor).

The drug guaifenesin is present in salt form and thus its solubility is higher in water and alcohols than in nonpolar solvents (heptane, hexane). Therefore, and taking into account the stationary phase solvent compatibility limitations, solute

Table 1. Geometrical Particle and Physical Parameters and Mobile Phase Density (ρ) and Viscosity (η)

Parameters	Chiralpak AD	*n*-Heptane/Ethanol (85/15)	
d_p [m]	20×10^{-6}	ρ [g/l]	η [cP]
ε_p	0.33	0.702	0.512

properties and considering literature results,[8] the mobile phases chosen was a *n*-heptane/ethanol mixture at 85/15 in volumetric percentage, which is a compromise between the separation requirements and viscosity (pressure drop) limitations. Moreover, the separation factor obtained for guaifenesin using this mobile phase was satisfactory for purposes of SMB separation without being necessary further tuning steps involving other solvents.

The CSP characteristics, as well as the mobile phase density and viscosity, are shown in Table 1.

Determination of Sorption Parameters and Validation

The physical and chemical parameters which specify a chromatographic system within each column of an SMB unit are essential to provide preliminary, and robust, design of a productive scale process. Therefore, the determination of sorption and hydrodynamic properties of the preparative column packed with chiral adsorbent through the experimental measurements is hereby described.

Single or multicomponent adsorption equilibrium isotherms are in fact the most relevant information for the design of an SMB separation. There are numerous methods for the adsorption equilibrium measurement and exhaustive reviews on this matter are available in the literature.[39] Over the years, several of these methods were tested at LSRE and one realized that reliable results could be easily obtained by means of the adsorption/desorption method.[40]

Materials and instrumentation

The GC-grade organic solvents *n*-heptane and ethanol (EtOH) were obtained from Sigma-Aldrich Chemie, Germany. Analyte guaiacol glyceryl ether (guaifenesine) was purchased from Sigma-Aldrich as well. A stainless steel column (250 mm $\times$ 4.6 mm I.D.) was packed with Chiralpak AD: amylose tris-(3,5 dimethylphenylcarbamate coated onto 20 μm silica-gel) and used to perform all adsorption experiments. An analytical column (250 mm $\times$ 4.6 mm I.D.) packed with Chiralpak IB: cellulose tris (3,5 dimethylphenylcarbamate immobilized onto 5 μm silica-gel), used for enantiomer samples analysis, was supplied by Chiral Technologies Europe (France). The antitussive drug guaifenesin was dissolved in the mobile phase which was always degassed and filtrated through a 0.2 μm, 50 mm I.D. NL 16-membrane filter (Schleicher & Schuell, Germany) before use. All the analyses were performed on a HPLC system which includes a Smartline 1000 LC pump, UV detector model Smartline 2500, LPG block, and degasser (Knauer, Germany). The detector was set at of 270 nm and a Rheodyne injection valve with a 10 μL sample loop was loaded manually using a syringe. Clarity (DataApex, 2004) software was used for data acquisition and HPLC control. All experiments were carried at ambient temperature ($\sim$25°C).

Determination of the multicomponent adsorption isotherms

The adsorption/desorption method was applied to obtain the guaifenesin competitive adsorption isotherms. Following this method, the preparative column was saturated with the excess of the racemic guaifenesin (feed solution) dissolved in the mobile phase at a known concentration. At the moment that equilibrium between the solute and the stationary phase was attained (long enough plateau) the column was regenerated with pure mobile phase. The total volume eluted from the column during the desorption step was collected and later analyzed in order to determine the concentration of each enantiomer.

Each single point of the adsorption isotherm for each enantiomer was calculated according to a known concentration of each enantiomer in the feed solution and in the eluted volume. The adsorption/desorption experiments were repeated for several different racemic guaifenesin feed concentrations.

The adsorbed amount of each enantiomer was calculated by using Eq. 1.

$$V_d C_i^d = \varepsilon_T V_c C_i^F + (1 - \varepsilon_T) V_c q_i \tag{1}$$

where the concentration of each enantiomer retained in the adsorbent, q_i (g/l) in equilibrium with the feed concentration, C_i^F (g/l), of the each compounds in the mobile phase. C_i^d, (g/l), is the concentration of species "i" in the desorbed volume, V_d (l), V_c (l) is the column volume and ε_T is the total porosity, obtained from column tracer experiments with nonadsorbable component (TTBB, 1,3,5-TriTert ButyBenzol) and related with the bulk porosity by $(\varepsilon_T = \varepsilon + (1 - \varepsilon)\varepsilon_p)$. The total loading capacity for the each concentration was calculated for the each feed concentration was calculated and a point of the adsorption isotherm obtained.

The equilibrium adsorption isotherms were determined in the feed concentration range of 1–10 g/l for racemic mixtures of guaifenesin in the mobile phase.

The CSP are usually considered having two types of the sites: selective and nonselective. In this work, we have also considered this fact and our first choice for the isotherm model was the modified Langmuir model or so-called linear + Langmuir isotherm. However, we have observed in the fitting procedure that the linear part of the isotherm, characterizing the nonselective sites, tends to zero and thus, the isotherm model reduces to simple multicomponent Langmuir isotherm model as given by Eq. 2, for the each species i,

$$q_i = \frac{q_m b_i C_i}{1 + \sum_{l=1}^{2} b_l C_l} \tag{2}$$

where b_i, b_l (l/g) are the adsorption constants for the adsorption of enantiomers i or l (A: S-enantiomer; B: R-enantiomer) on the enantioselective sites and q_m (g/l) is the saturation capacity of the enantioselective sites. The adsorption constant at

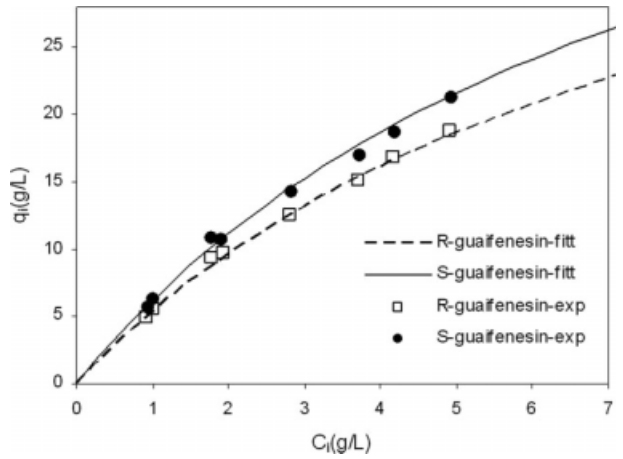

Figure 2. Competitive adsorption equilibrium of guaifenesin onto Chiralpak AD.

infinitive dilution, K_i, for each enantiomer is defined as follows, Eq. 3.

$$K_i = q_m b_i \tag{3}$$

To obtain a thermodynamically consistent adsorption isotherm model, the saturation capacity of the enantioselective sites was assumed to be equal for both enantiomers. The adsorption isotherm of guaifenesin onto Chiralpak AD is shown on Figure 2.

The adsorption isotherm parameters were estimated using Levenberg-Marquardt algorithm, summarized in Table 2.

Using the data from Table 2, the calculated selectivity is 1.16, which can be classified as a hard separation in terms of difficulty (considering a hard separation: selectivity = 1.10; moderate separation: selectivity = 1.50, and easy separation: selectivity = 4.00). This value gives reduced peaks resolution and thus an increased difficulty to obtain pure enantiomers by means of batch chromatography modus operandi.

Validation of the sorption parameters by means of frontal Analysis

To verify the competitive adsorption equilibrium isotherm for guaifenesin, several adsorption and elution experiments, using different feed concentration, were performed. All experiments were carried out in a stainless steel column (250 mm × 4.6 mm I.D.) packed with Chiralpak AD with 20 μm particles. The racemic solution of guaifenesin was prepared in the mobile phase of *n*-heptane/ethanol (85/15%, v/v) in order to avoid any concentration gradient during the measurement. The total feed concentration of 2, 4, and 8 g/l, at ambient temperature (25°C) and flow rate of 1.5 ml/min was used. The column was being saturated with the feed solution of guaifenesin until the concentration in the outlet of the column attained the feed concentration and the UV detector displayed long enough plateau. Afterwards, the pure mobile phase was passed through the column in order to obtain the desorption profile of guaifenesin. During the entire saturation and elution steps, the samples were withdrawn at the outlet of the column at the certain time periods. All collected samples were quantitatively analyzed using an analytical column packed with Chiralpak IB (particle size 5 μm). The mobile phase used for the analysis procedure was *n*-heptane/ethanol (60/40%, v/v).

The adsorption and desorption profiles for guaifenesin obtained for a stainless steel column (250 mm × 4.6 mm I.D.) packed with Chiralpak AD (20 μm particles) at different feed concentrations are shown in Figure 3. The experimental profiles of guaifenesin were compared with the mathematical model given in Appendix A, which considers the following assumptions: axial dispersed plug flow, internal mass-transfer resistances for the absorbable species described by a linear driving force model, isothermal operation, and constant particle size and packing porosity.

The experimental adsorption and desorption profiles are in very good agreement with the simulation results in the considered concentration range. Because the correctness of the adsorption equilibrium isotherm for guaifenesin was verified, the SMB design, and operation was carried on.

Modeling and Design of the SMB Unit

The SMB mode of operation can be easily described by means of an equivalent TMB apparatus, while a TMB represents a continuous chromatographic separation technique involving a counter-current movement of the stationary against a liquid phase, Figure 4 (a). In the SMB, this solid counter current movement is simulated by shifting all inlet and outlets ports at discrete time intervals (switching time) in the direction of the fluid phase, Figures 4b,c.

Similarly to what happens in the TMB approach, also each section in the SMB unit plays a different role in the whole separation process; nevertheless, in the SMB the columns that constitute these sections change over the time.

Modeling strategy

Generally, an SMB unit can be modeled by means of two different approaches: the "equivalent" TMB and the "real" SMB approach.[41] The equivalence between the TMB and the SMB approaches is obtained by keeping constant the liquid interstitial velocity relative to the solid interstitial velocity. This equivalence when expressed in terms of interstitial velocities becomes: $v_j = v_j^* - u_s$, where $u_s = \frac{L_c}{t^*}$, is the solid velocity in TMB, $v_j = \frac{Q_j}{\varepsilon A_c}$ is the interstitial liquid velocity in the TMB and v_j^* in the SMB, A_c is the cross section area of the bed, Q_j is the TMB liquid flow rate, and ε is the bed porosity. This equivalence expressed in terms of SMB and TMB flow rates is given by: $Q_j^* = Q_j + \frac{\varepsilon}{1-\varepsilon} Q_s$ with $Q_s = \frac{(1-\varepsilon)V_c}{t^*}$, where Q_j^* is the liquid flow rate in section j of the SMB, Q_s is the TMB solid flow rate, and V_c is the volume of one SMB column.

Although the "equivalent" TMB modeling approach provides continuous solutions (leading to Steady State solutions), avoiding a considerable computation time, it just

Table 2. Multicomponent Adsorption Isotherm Parameters

q_m [g/l]	b_A [l/g]	b_B [l/g]	K_A	K_B
106.759	0.065	0.056	6.939	5.978

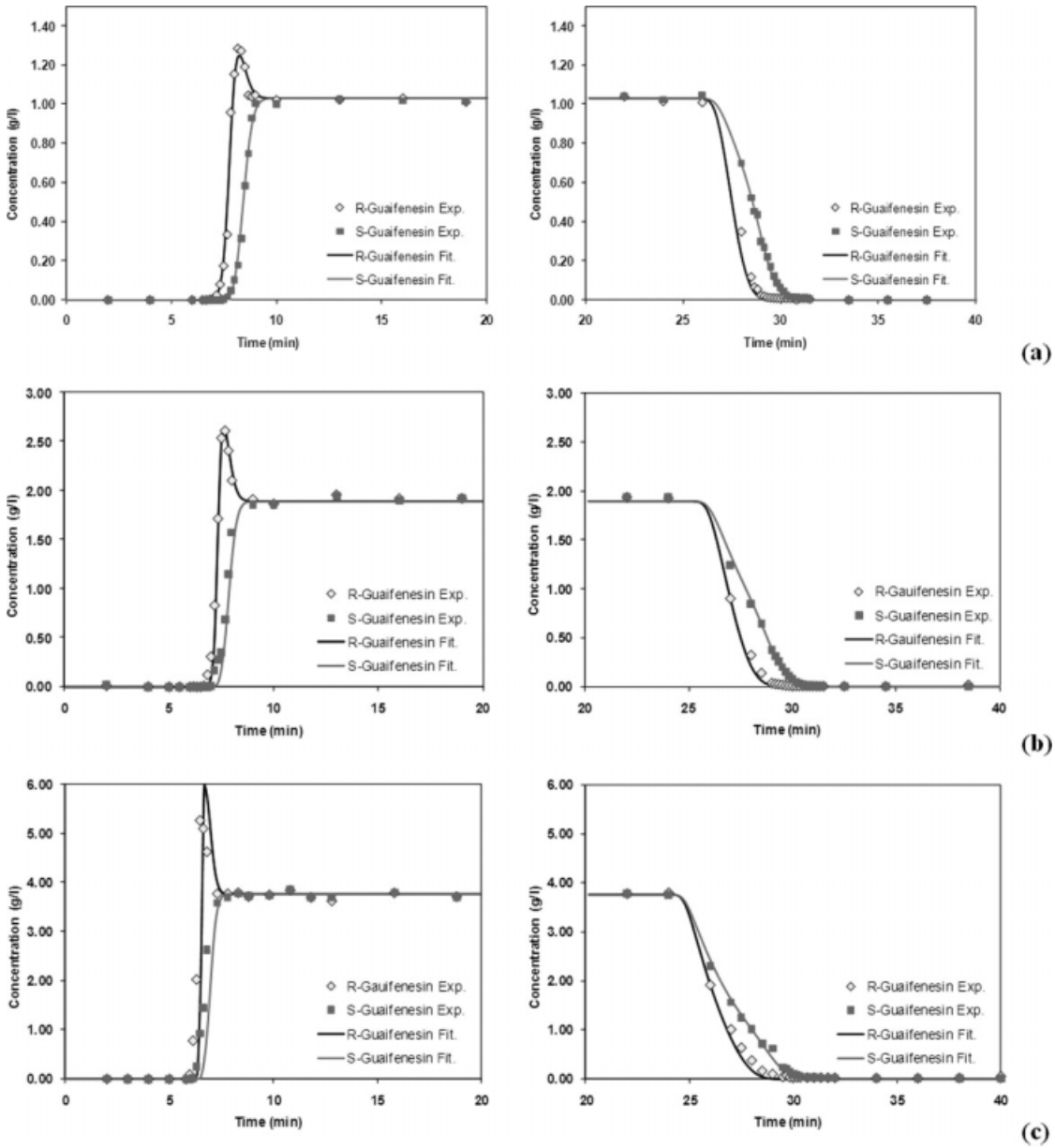

Figure 3. (a) Adsorption and (b) desorption curves of enantiomers of guaifenesin at the feed concentration of racemate of: (a) 2.0 g/l; (b) 4.0 g/l; and (c) 8.0 g/l (flow rate 1.5 ml/min).

gives satisfactory results (close to the real SMB unit) when a large number of columns per section is considered. The "real" SMB modeling approach considers the ports discontinuities, simulating in fact, as the SMB unit apparatus, the solid movement and thus, reaching a Cyclic Steady State (CSS). This second methodology is quite more accurate and hence will be used in this work. An axial dispersion flow for the liquid phase, linear driving force (LDF) for the intraparticle mass transfer rate and multicomponent adsorption equilibrium described by the previously mentioned Langmuir isotherm are considered in the model.

The SMB model equations are similar to those established for the fixed bed experiments (see Appendix A), but now set for each column k in each section j for each species i, and thus, by performing a mass balance to a volume element of the column k, becoming,

$$\varepsilon\frac{\partial C_{ik}}{\partial t}=\varepsilon D_{\mathrm{L}k}\frac{\partial^2 C_{ik}}{\partial z^2}-\varepsilon v_k^*\frac{\partial C_{ik}}{\partial z}-(1-\varepsilon)\frac{3}{r_{\mathrm{p}}}k_{\mathrm{int}_i}(C_{ik}-C_{\mathrm{p}_{ik}}) \quad (4)$$

and similarly the particle mass balance,

$$\varepsilon_{\mathrm{p}}\frac{\partial C_{\mathrm{p}_{ik}}}{\partial t}+(1-\varepsilon_{\mathrm{p}})\frac{\partial q_{ik}}{\partial t}=\frac{3}{r_{\mathrm{p}}}k_{\mathrm{int}_i}(C_{ik}-C_{\mathrm{p}_{ik}}) \quad (5)$$

with the initial conditions:

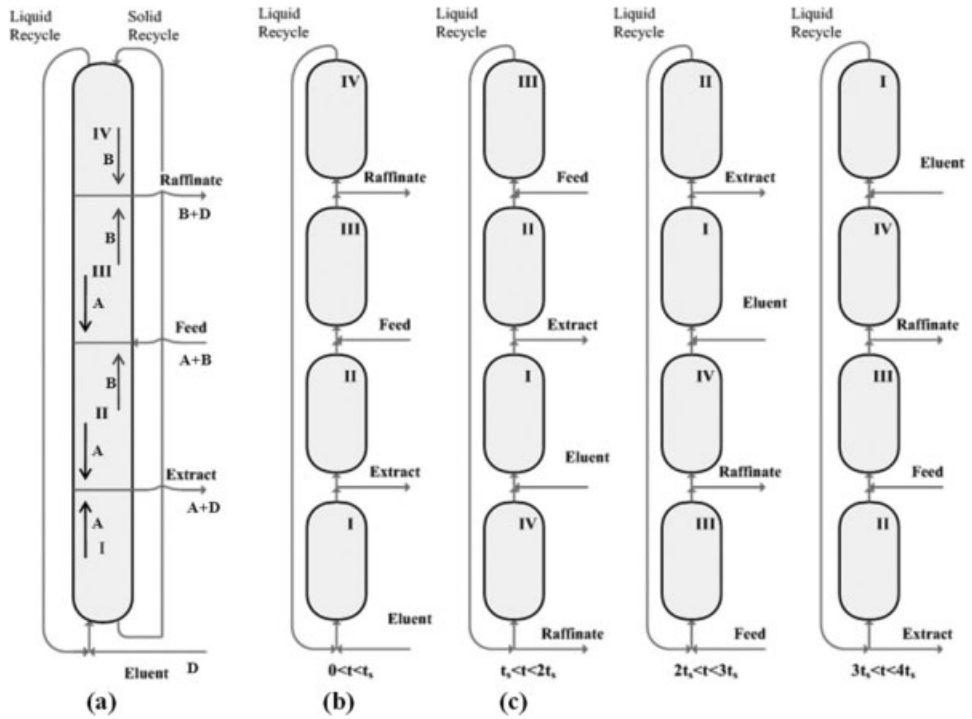

Figure 4. Schematic representation of a 4 columns SMB unit operating over a complete cycle, from 0 to 4*t* (with *t*** representing the ports switching time); (a) period of the first switch; (b) period of the second switch; and (c) TMB unit.**

$$t = 0: \; C_{ik} = C_{\mathrm{p}_{ik}} = q_{ik} = 0 \tag{6}$$

The Danckwerts boundary conditions at the inlet of column ($z = 0$) and column exit ($z = L_k$) for ($t > 0$) are set for each column k,

$$z = 0: \; D_{\mathrm{L}k}\frac{\partial C_{ik}}{\partial z} = v_k^*(C_{ik} - C_{ik}^{\mathrm{in}}) \tag{7a}$$

$$z = L_k: \; \frac{\partial C_{ik}}{\partial z} = 0 \tag{7b}$$

The adsorption equilibrium isotherm described by Eq. 2, becomes:

$$q_{ik} = f(C_{\mathrm{p}_{ik}}) \tag{8}$$

The fluid velocities and inlet concentrations in each section j are calculated from the inlet and outlet streams nodes balances, defined by the following equation during the first switch time (from 0 to t^*) becoming:

In the extract (X) node

$$v_{\mathrm{I}}^* - v_{\mathrm{X}} = v_{\mathrm{II}}^* \tag{9a}$$

$$C_{i\mathrm{Nc}_I}^{\mathrm{out}} = C_{i(\mathrm{Nc}_I+1)}^{\mathrm{in}} = C_{\mathrm{iX}} \tag{9b}$$

In the raffinate (R) node:

$$v_{\mathrm{III}}^* - v_{\mathrm{R}} = v_{\mathrm{IV}}^* \tag{10a}$$

$$C_{i(\mathrm{Nc_I}+\mathrm{Nc_{II}}+\mathrm{Nc_{III}})}^{\mathrm{out}} = C_{i(\mathrm{Nc_I}+\mathrm{Nc_{II}}+\mathrm{Nc_{III}}+1)}^{\mathrm{in}} = C_{\mathrm{iR}} \tag{10b}$$

In the feed (F) node:

$$v_{\mathrm{II}}^* + v_{\mathrm{F}} = v_{\mathrm{III}}^* \tag{11a}$$

$$C_{i(\mathrm{Nc_I}+\mathrm{Nc_{II}})}^{\mathrm{out}} v_{\mathrm{II}}^* + C_{\mathrm{iF}} v_{\mathrm{F}} = C_{i(\mathrm{Nc_I}+\mathrm{Nc_{II}}+1)}^{\mathrm{in}} v_{\mathrm{III}}^* \tag{11b}$$

And in the eluent (E) node:

$$v_{\mathrm{IV}}^* + v_{\mathrm{E}} = v_{\mathrm{I}}^* \tag{12a}$$

$$C_{i(\mathrm{Nc_I}+\mathrm{Nc_{II}}+\mathrm{Nc_{III}}+\mathrm{Nc_{IV}})}^{\mathrm{out}} v_{\mathrm{IV}}^* = C_{\mathrm{iI}}^{\mathrm{in}} v_{\mathrm{I}}^* \tag{12b}$$

And for the remaining columns (not considered in the borders of the sections),

$$C_{ik}^{\mathrm{out}} = C_{i(k+1)}^{\mathrm{in}} \tag{13}$$

where Nc_j represents the total number of columns in section j.

Numerical solution of model equations

The mathematical model involves a system of partial differential and algebraic equations that was solved using the gPROMS software package (version 3.0.4) from Process System Enterprise (UK). The numerical method used was based on the orthogonal collocation in finite elements (OCFEM) with an axial discretization in 40 finite elements per column, with two interior collocation points. An absolute and relative tolerance was set to 10^{-5}.

SMB performance parameters

The performance of the SMB unit for the separation of a binary mixture (racemic mixture) can be characterized by the following parameters: purity, recovery, and productivity per unit of the adsorbent volume. The definitions of the SMB performance parameters considered in this work are given bellow:

Purity (%) of S-guaifenesin (A) in extract and R-guaifenesin (B) in raffinate stream:

$$PU_X = \frac{\int_t^{t+6t^*} C_{AX}dt}{\int_t^{t+6t^*} C_{AX}dt + \int_t^{t+6t^*} C_{BX}dt} \tag{14a}$$

$$PU_R = \frac{\int_t^{t+6t^*} C_{BR}dt}{\int_t^{t+6t^*} C_{BR}dt + \int_t^{t+6t^*} C_{AR}dt} \tag{14b}$$

Recovery (%) of S-guaifenesin in extract (A) and R-guaifenesin (B) in raffinate stream:

$$Re_X = \frac{\int_t^{t+6t^*} C_{AX}dtQ_X}{6t^*Q_F C_{AF}} \tag{15a}$$

$$Re_R = \frac{\int_t^{t+6t^*} C_{BR}dtQ_R}{6t^*Q_F C_{BF}} \tag{15b}$$

Productivity expressed in grams of pure enantiomers (in the extract or the raffinate streams) per volume of CSP per day ($g_{enantiomer}/(dm^3$ CSP day)):

$$PR_X = \frac{\int_t^{t+6t^*} C_{AX}dtQ_X}{6t^*V_c(1-\varepsilon)\sum_{j=1}^{IV} Nc_j} \tag{16a}$$

$$PR_R = \frac{\int_t^{t+6t^*} C_{BR}dtQ_R}{6t^*V_c(1-\varepsilon)\sum_{j=1}^{IV} Nc_j} \tag{16b}$$

SMB design methodology

The design of an SMB separation involves taking decisions at many levels, starting from the configuration of the unit (number of columns per section, column, and particle size) finishing with the selection of the operating conditions (feed concentration, switching time, internal flow rates). Although simulation work can be exhaustively done until the right combination of the above parameters for the expected SMB performance is found, it is useful to have a design method that will provide a preliminary estimation of the operating point, followed by simulation (and/or optimization) and refinement. In this work, the number of columns and their geometry were previously selected. One can now focus on the operating conditions. Recalling the role of each section (Figure 4), one can enunciate some constraints that will limit the feasible region for the complete separation (recovery of the more retained species (A) in the extract stream and a less retained one (B) in the raffinate port, corresponding to the arrows in Figure 4a). In particular, we can set the net fluxes for each component in each of the four sections so that the more retained species is directed upwards in Section I, ensuring solid phase regeneration; in Sections II and III, the species movement is directed downwards for the more retained and upwards for the less retained one; and in Section IV, the less retained species should move downwards, ensuring regeneration of the eluent to be recycled. These net flow rate constraints define both the separation region (Section II and III), as the regeneration one (Section I and IV).

$$\gamma_I > \frac{1-\varepsilon}{\varepsilon}\frac{\langle n_{AI}\rangle}{C_{AI}} \tag{17a}$$

$$\frac{1-\varepsilon}{\varepsilon}\frac{\langle n_{BII}\rangle}{C_{BII}} < \gamma_{II} < \frac{1-\varepsilon}{\varepsilon}\frac{\langle n_{AII}\rangle}{C_{AII}} \tag{17b}$$

$$\frac{1-\varepsilon}{\varepsilon}\frac{\langle n_{BIII}\rangle}{C_{BIII}} < \gamma_{III} < \frac{1-\varepsilon}{\varepsilon}\frac{\langle n_{AIII}\rangle}{C_{AIII}} \tag{17c}$$

$$\gamma_{IV} < \frac{1-\varepsilon}{\varepsilon}\frac{\langle n_{BIV}\rangle}{C_{BIV}} \tag{17d}$$

where $\langle n_{ij}\rangle$ is the total average solid concentration of species i in section j, with $\langle n_{ij}\rangle = (1-\varepsilon_p)q_{ij} + \varepsilon_p C_{p_{ij}}$, and $\gamma_j = \frac{v_j}{u_s}$, the ratio between the fluid and solid interstitial velocities.

Equilibrium Assumptions. The identification of the constraints mentioned above (Eqs. 17) led to the appearance of several design methods, which are usually approximations but allowing graphical schemes, providing a better visualization of the separation regions. For instance, the relation $\frac{\langle n_{ij}\rangle}{C_{ij}}$ can be simplified by assuming that the adsorption equilibrium is established everywhere at every time (from the Equilibrium Theory assumptions), resulting in a feasible separation region defined by constraints given by Eqs.17b and 17c, which in the case of linear isotherms takes the shape of a rectangular triangle when presented in the $\gamma_{II} \times \gamma_{III}$ plane, the so-called Triangle Theory.[42] The Equilibrium Theory approximation can be also used for preliminary calculation of the operating conditions in Sections I and IV. For the separation hereby analyzed, the maximum flow rate in Section I was set at 41 ml/min (a compromise between the hardware limitation and pressure drop restriction, around 45 ml/min, in the FlexSMB-LSRE® unit). According to the Equilibrium Theory for a complete regeneration of the solid phase in Section I,[43] the following condition must be fulfilled,

$$\gamma_I > \gamma_{Imin} = \frac{1-\varepsilon}{\varepsilon}(K_A(1-\varepsilon_p)+\varepsilon_p) = 7.47 \tag{18}$$

where $K_A = 6.94$ is the initial slope of the isotherm of the more retained compound and by consequence the switching time (t^*) that will fulfil this condition can be 2.57 min.

As explained before, the purpose of Section IV is to regenerate the liquid phase, thus the less retained compound

must move towards the raffinate port. The SMB flow rate in the Section IV was calculated according the following equation:

$$Q^*_{IV} = \frac{\varepsilon V_c}{t^*}\left(1 + \frac{1-\varepsilon}{\varepsilon}\left(\varepsilon_p + (1-\varepsilon_p)\frac{\Delta q^F_B}{\Delta C^F_B}\right)\right) \quad (19)$$

where $\frac{\Delta q^F_B}{\Delta C^F_B}$ is the slope of the less retained compound and $V_c = 31.4$ cm^3, the column volume used for this separation. Considering a concentration of the less retained compound in the feed of 2 g/l then the term $\frac{\Delta q^F_B}{\Delta C^F_B}$ is then equal to 5.38 consequently the flow rate in the Section IV 33.8 ml/min. For this value of the flow rate and the selected switching time, the condition for complete eluent regeneration in Section IV is fulfilled: $\gamma_{IV} < \gamma_{IV_{max}} = \frac{1-\varepsilon}{\varepsilon}(K_B(1-\varepsilon_p)+\varepsilon_p) = 6.50$, stated by Equilibrium Theory for the Section IV, is fulfilled.

The separation region for equilibrium assumption obtained by the procedure suggested by Mazzotti et al.[43] is presented in Figure 5.

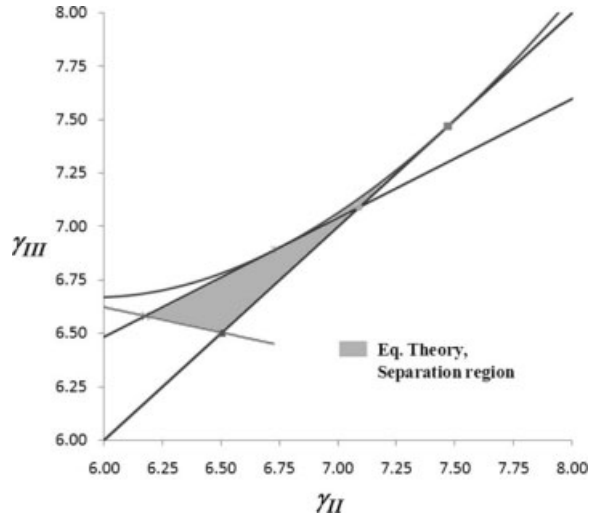

Figure 5. Separation region deffined according with the Equilibrium Theory assumptions (Triangle Theory).

As can be observed in Figure 5, the separation region for the guaifenesin enantiomers has a triangular shape in $\gamma_{II} \times \gamma_{III}$, characteristic of the systems with a weak desorbent (eluent). According to the Equilibrium Theory assumptions, a point within this separation region gives the operating conditions which provide complete separation (pure extract and raffinate). Nevertheless, the real units generally do not fulfil the Equilibrium Theory assumption.

Including Mass Transfer Resistances and Real Unit's Particularities. The design assumptions used in the SMB model approach do not account neither for the mass transfer resistances, nor for real SMB unit's particularities (i.e., tubing and equipment dead volumes, switching time asymmetries and delays, pumps flow rates variations, and equipment limitations).

It is well known that a robust unit design should consider the mass transfer resistances.[44] Based on the model given in the previous section, it is possible to construct a more accurate separation region, which will account for the several aspects described in the model. This is done by successive simulation of different $\gamma_{II} \times \gamma_{III}$ pairs. When significantly higher values for γ_I and lower values for γ_{IV} than the ones predicted by the triangle theory are considered, the regeneration region does not influence the shape and size of the separation region, as stated by the separation volume concept.[44]

In addition, it should be taken into account that the performance of a real SMB unit differs from the ones described by the commonly used modeling and design strategies. There are several factors that can influence the precision of the SMB model predictions, such as: uncertainty in adsorption equilibrium kinetics and hydrodynamics data (diffusivity, axial dispersion coefficients, etc.) and bed voidage (packing asymmetries), as well as, extra column dead volumes (tubing, equipment, asymmetries), variation in the port switching velocity (asymmetries and delays), fluctuations in pump flow rates (fluid inlets, outlets, and internal), which are not accounted for it in the most commonly used SMB models.[45] Consequently, if one runs an experimental SMB unit based on the operating parameters obtained by a simple mathematical model, such as the one described in the previous section, the experimental results may not match the ones that were predicted by the model.

Concerning the uncertainty in the equilibrium isotherm data, kinetics data, and even the asymmetries of columns packing, the more precise, and/or accurate, these factors are, the better will be the SMB model predictions. Therefore, detailed and precise measurements of all these parameters have to be done a priori, so that they introduce a minimal discrepancy between the SMB model results and the experiments itself.

The remaining deviation factors, such as the tubing and equipment dead volumes, pumps, and valves asymmetries, related to each SMB unit design and equipment particularities should be taken into account before starting to construct a new SMB unit.

Before the unit design and construction. The FlexSMB-LSRE® unit was designed to minimize deviation aspects related to common SMB unit design. To minimize the extra column dead volumes (tubing, equipment, asymmetries), the tubing and equipment dead volumes were reduced by using of 1 mm i.d. tubes and short dead end (SD, Valco Instruments) valves. To reduce the dead volumes asymmetries, tubes with the same length were used for the same function and all columns assembled unit in carousel, Figure 6.

To reduce the pumps flow rates fluctuations (fluid inlets, outlets, and internal), HPLC pumps were used, assisted with Coriolis flow meters. Purge valves after each pump, to avoid pressuring during the valves switching step, were used. These valves can also be used to regulate the total system pressure, as well as security valves.

Although small variations in the internal flow rates at large-scale SMB units are relatively easy control, the use of a recycle pump in a small-scale SMB systems (like for example, the Licosep 12-26, see Appendix B) introduces extra dead volumes and system asymmetry that could lead to a considerable decrease in the product purities.[46] The unit asymmetry issues may be solved by using a more elaborated pumps and valves configurations (i.e., more complex design schemes) with a possibly for asynchronous shift of inlets and

Figure 6. The FlexSMB-LSRE® unit assembled with six columns.

outlets; solution implemented by Separex (now Novasep, France) in the Licosep 12-26 unit.[33,47]

The FlexSMB-LSRE® unit uses two SD valves per stream for the extract and raffinate stream and one SD valve per stream for the feed and eluent/desorbent streams. Also one two-way valve per column is used, similar to the Negawa and Shoji configuration (US Patent 5,456,825, 1995). There is just one pump within the main system line, always connected to the extract line.

On this way, asymmetries related with the recycle pump are avoided. Most important advantage of the FlexSMB-LSRE® is that can operate in the most of the nonconventional SMB operating modes with a simple adjustment and columns reconfiguration, Figure 7.

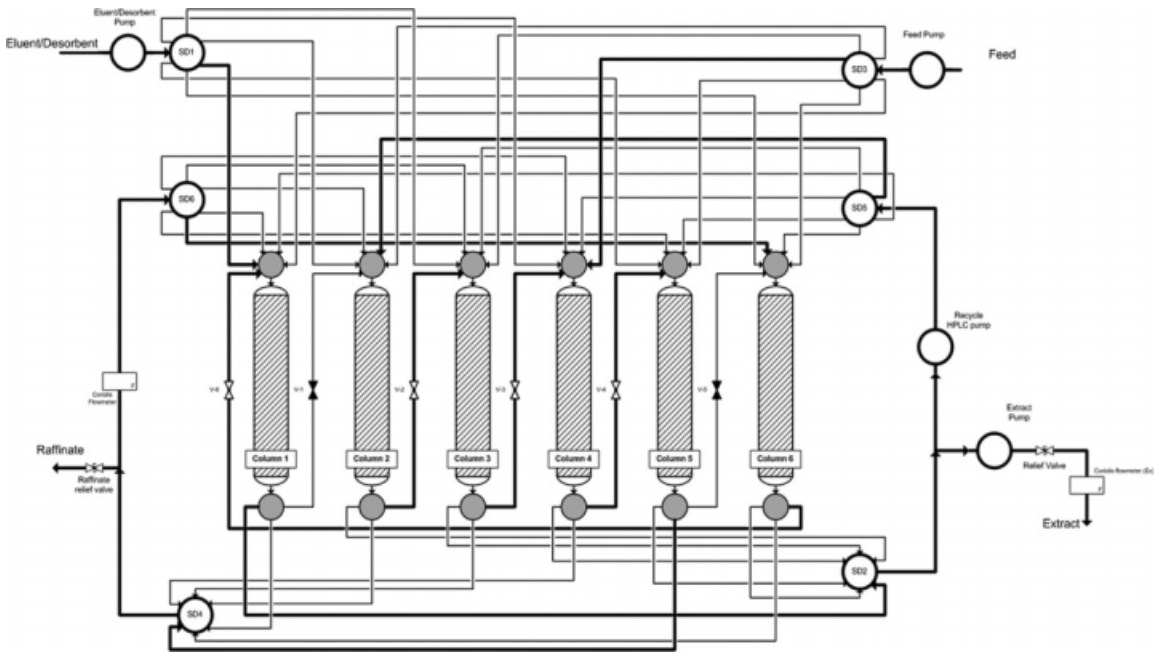

Figure 7. FlexSMB-LSRE® pumps and valves scheme, during the first step, six columns configuration to operate a [1 2 2 1] classic SMB.

Bold lines are the active connections; thick lines are stagnant volumes.

Table 3. Dead Volumes Per Function and Total Dead Volumes Percentage in the FlexSMB-LSRE® Unit

	V_{each} (ml)	Total
Fritz and manifold	0.50	3.01
Ext in	0.36	2.17
Raf in	0.36	2.17
Ext out	0.32	1.93
Raf out	0.32	1.93
Interc	0.31	1.89
Sampler	0.47	0.47
Ext 1	0.12	0.12
Ext 2 (Rec pump)	3.93	3.93
Raf 1	0.12	0.12
Raf 2 (flow meter)	6.67	6.67
		20.40
V_c^* (ml)		188.5
(%) Dead volumes		11.5%

*Considering six columns of 10 cm height and 2 cm of i.d.

To avoid variations related to the ports switching velocity asymmetries a distributed connection scheme for SD valves was used. The FlexSMB-LSRE® can operate with a maximum number of columns of 12. The columns were connected to the 12 ways SD valves using the odd valve connecting positions (i.e., 1, 3, …, 9, 11) in order to reduce the switching time discrepancies (see Figure 6).

After the unit design and construction, operation. Even after all the work done concerning the system dead volumes and operation asymmetries:

(a) The unit still has 11.5% of dead volumes, Table 3.

The values given in Table 3 include also the value of the stagnant volumes. Considering only the active lines (see Figure 7), the dead volumes for each section are: $V_{\mathrm{I}}^{\mathrm{D}} = 1.09$ ml; $V_{\mathrm{II}}^{\mathrm{D}} = 5.48$ ml; $V_{\mathrm{III}}^{\mathrm{D}} = 1.71$ ml; $V_{\mathrm{IV}}^{\mathrm{D}} = 7.61$ ml.

(b) The port switching velocity variation (delay) can represent around 0.5% of the switching time (0.8 s); with a six columns apparatus: 1 complete switch = switch + 0.4 s hold (zero flow rates) + switch;

(c) The fluctuation of the pumps flow rates are still considerable, Figure 8.

If the average internal flow rates in each section are kept constant during the SMB operation (as assumed by some SMB design procedure) the SMB performances would not be affected, despite their considerable local variations shown in Figure 8. This is due to the cyclic mode of operation of these units, leading to compensation of these variations with time.

However, there are still two major issues concerning the prediction of the SMB performances: the unit SMB design features related with the dead volumes and the switching time asymmetries or delay. To deal with discrepancies between the real SMB operation and that predicted with commonly used models that account only for the presence of SMB columns (and do not consider the surrounding equipment features) one can apply two different compensation strategies, a priori or a posteriori:

(i) a priori compensation strategy. Predict the operating parameters by means of the regular SMB models and then apply a compensation measure during the unit operation (to account with the units' discrepancies from the used model);

(ii) a posteriori compensation strategy. Use a detailed SMB model by including as more units' particularities as possible.

The first strategy (i) is represented, for instance, by the asynchronous port shift in the Licosep units, discussed,[33,34,47] and hereby simplified by switching time compensating strategy, see details in Appendix B. The second strategy (ii) was discussed by several authors, within the Triangle Theory spectrum,[35,48] or in the case of the Standing Wave Theory.[45,49]

One can now analyze both situations. For that purpose, a detailed model was applied to the FlexSMB-LSRE® unit accounting for its tubes and equipment dead volumes, filters (fritzs), and manifold as well as the switching asymmetries (or switching time delay), as presented in Figure 9.

Similarly to what is mentioned in Appendix B for the Licosep SMB unit, all dead volumes are modeled by an axial dispersive plug and flow approach and the switching time discontinuities detailed.

By running successive simulations for different $\gamma_{\mathrm{II}}^* \times \gamma_{\mathrm{III}}^*$ pairs, it is possible to draw the "true" separation region for the case of gaufenesin separation (case study in this work). In Figure 10 are shown the Equilibrium Theory, SMB-zero dead volumes and the FlexSMB-LSRE® (the extended model as stated in Figure 9).

As can be observed from Figure 10, the separation region obtained with the dead volumes and switching time asymmetries respecting the FlexSMB-LSRE® unit, appears shifted from those obtained with the Equilibrium Theory and SMB-zero dead volumes model. The SMB-zero dead volume separation region is slightly larger than that calculated by the Equilibrium Theory. This difference is due to the different product purities in both cases, minimum 99% in the SMB-zero dead volume model and 100% from the Equilibrium Theory.

Let us now make use of the SMB-zero dead volumes separation region and correct it to account with the unit dead volumes by shifting it using the following equation:

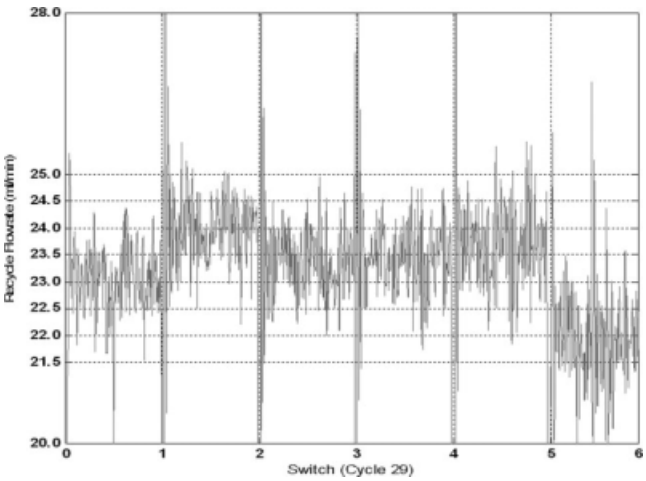

Figure 8. Variation of the recycle flow rate during complete cycle for a six columns SMB, test done with pure eluent mixture of *n*-heptane/2-propanol (95/5% v/v).

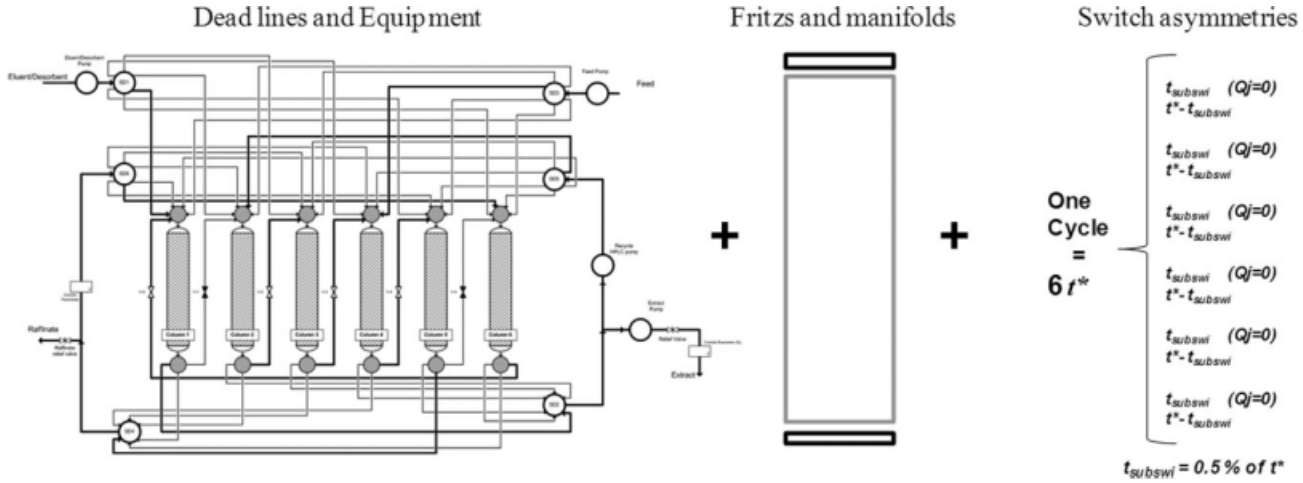

Figure 9. Schematic illustration for the unit particularities included in the detailed FlexSMB-LSRE® model.

$$\gamma_j^*|_{\text{FlexSMB}} = \gamma_j^*|_{\text{SMB}} + \frac{1-\varepsilon}{\varepsilon}\frac{\langle V_j^{\text{D}}\rangle_{\text{II,III}}}{V_{\text{c}}(1-\varepsilon)} \tag{20}$$

$$t^*|_{\text{FlexSMB}} = t^*|_{\text{SMB}} + \frac{\sum_{j=1}^{IV} V_j^{\text{D}}}{\bar{Q}_j^*}\frac{1}{\sum_{j=1}^{IV} Nc_j} \tag{21}$$

This procedure is similar to the one proposed by Migliorini et al.[35] (recently detailed to account for each section connection lines and respective volumetric flow rate[48]), but simplified for Sections II and III by using the average dead volumes of these sections $\langle V_j^{\text{D}}\rangle_{\text{II,III}} = \frac{1}{2}(V_{\text{II}}^{\text{D}} + V_{\text{III}}^{\text{D}})$. We call this a priori compensation procedure: "SMB with Design" (the design accounts for dead volumes compensation).

The second a priori compensation strategy proposed in our work is the switching time compensating measure described in Appendix A, hereby called switching time compensation.

Both a priori compensation strategies were used to correct the SMB-zero dead volumes separation region and compare it with the one obtained using the a posteriori compensation strategy, that is, detailed FlexSMB-LSRE® model, Figure 11.

As can be observed from Figure 11, both the "SMB with Design" and the switching time compensation strategies shifted up the SMB-zero dead volumes separation region near to the FlexSMB-LSRE® separation region. However, the separation region obtained after applying the switching

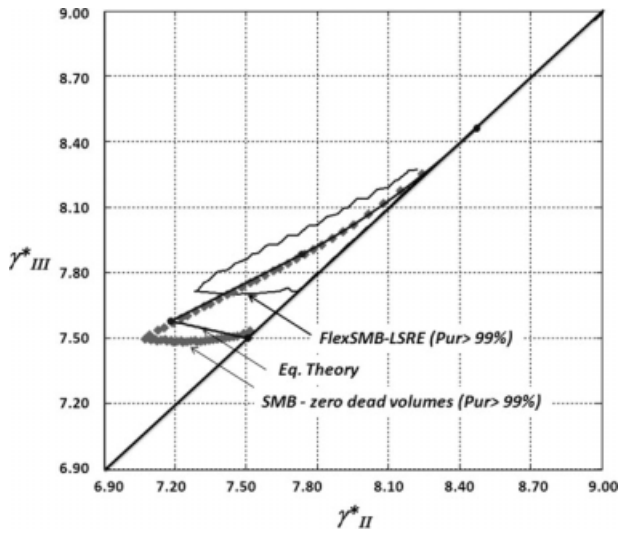

Figure 10. Separation regions according to the Equilibrium Theory, SMB zero dead volumes and the FlexSMB-LSRE®, the last two obtained for a minimum purity requirement of 99% in both extract and raffinate.

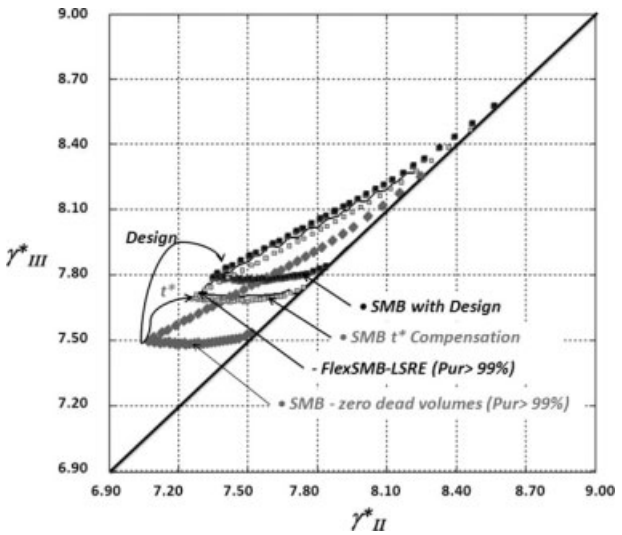

Figure 11. Comparison between the separation regions obtained with the a priori (Switching time and "SMB with design") compensating measures and a posteriori compensation (detailed FlexSMB-LSRE® model) measure.

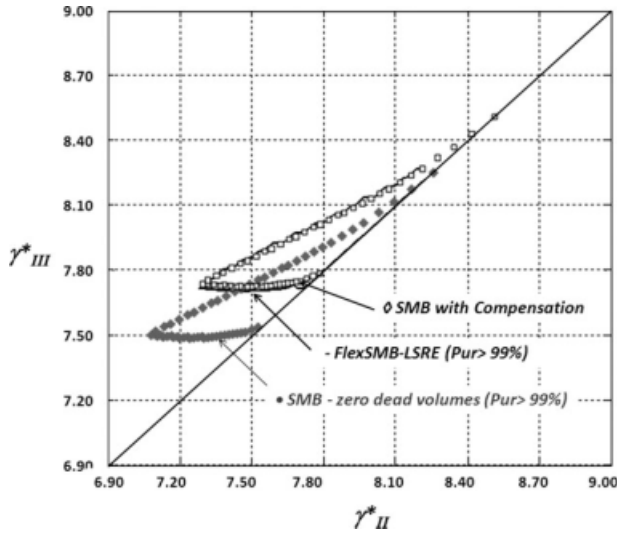

Figure 12. Separation region obtained by the extended switching time compensation measure (corrected by the subswitch interval).

time compensating measure is closer to the FlexSMB-LSRE® separation region than that obtained with the "SMB with Design" strategy. The last one could be improved, by detailing the compensation to each section and using more elaborated procedures.[48] However, due to its simplicity, the switching time compensating measure would be preferred.

The switching time compensating measure accounts only for equipment dead volumes, the switching time delay, or asymmetry is still not compensated when this measure is used. They can be included in the switching time compensation measure as true delay in the switching time, by extending Eq. 22 as follows:

$$t^*|_{\text{FlexSMB}} = t^*|_{\text{SMB}} + \frac{\sum_{j=1}^{IV} V_j^{\text{D}}}{\overline{Q_j^*}} \frac{1}{\sum_{j=1}^{IV} Nc_j} + t_{\text{subswitch}} \quad (22a)$$

Table 4. Experimental Operating Conditions of the SMB Experiment

No. Columns: 6		External Porosity, $\varepsilon = 0.4$	
Configuration: 1:2:2:1		Feed Concentration:	
Columns: Length: 10 cm;		4.0 g/dm^3 (racemate)	
Diameter: 2.0 cm		Particle Size: 20 μm	
SMB Condition			
Section I	43.0 cm^3/min	Eluent	10.5 cm^3/min
Section II	36.3 cm^3/min	Extract	6.7 cm^3/min
Section III	37.2 cm^3/min	Feed	0.9 cm^3/min
Section IV	32.5 cm^3/min	Raffinate	4.7 cm^3/min
t^* 2.65 min			
$\gamma_{\text{I}}^*\|_{\text{FlexSMB}}$ = 9.06	$\gamma_{\text{II}}^*\|_{\text{FlexSMB}}$ = 7.65	$\gamma_{\text{III}}^*\|_{\text{FlexSMB}}$ = 7.84	$\gamma_{\text{IV}}^*\|_{\text{FlexSMB}}$ = 6.85

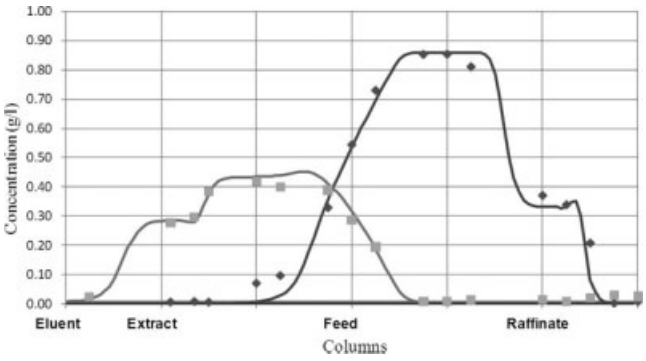

Figure 13. Experimental internal concentration profile at the cyclic steady state (CSS) for feed concentration of 4.0 g/dm^3 (racemate).

And for the FlexSMB-LSRE®:

$$t^*|_{\text{FlexSMB}} = t^*|_{\text{SMB}}(1 + 2.6\% + 0.5\%) \quad (22b)$$

where $t^*|_{\text{SMB}}$ represents the switching time for a ideal SMB unit with zero dead volumes, V_j^{D}, the total dead volumes in section j, $\overline{Q_j^*} = 38.5$ ml/min, the unit's average flow rate, and $t_{\text{subswitch}}$, the sub switching time delay (see Figure 9).

The corrected separation region using the extension to the switching time compensating measure is shown in Figure 12.

As can be observed in Figure 12, the SMB-zero dead volumes separation region corrected by the dead volumes and switching time delay (asymmetries) almost matches the one obtained with the detailed model. By this means, it is possible to easily obtain a precise and realistic separation region without running tedious simulations related with the more detailed SMB models.

One can now improve the estimation based on the Equilibrium Theory assumptions (Section 4.4.1) to obtain corrected operating conditions that will account for the mass transfer resistances and the particular unit dead volumes and switching time delay.

The volumetric flow rates in Sections I and IV (41 ml/min and 34 ml/min, respectively) were recalculated to account with a safety factor that will avoid contamination due to mass transfer effects. In this case, the flow rate in Section I was increased for 5% and in Section IV was decreased for 5%: $Q_{\text{I}}^* = 43$ ml/min and $Q_{\text{IV}}^* = 32.5$ ml/min.

From the separation region presented in Figure 5, $(\gamma_{\text{II}} = 6.375; \gamma_{\text{III}} = 6.575)$ was selected, away from the triangle limits to avoid products pollution as consequence of the mass transfer effects. The switching time was corrected according to Eq. 22b and the new value is 2.65 min. The

Table 5. Simulated and Experimental Purities and Recoveries During the 29th Cycle

	Simulated		Experimental	
	Extract (%)	Raffinate (%)	Extract (%)	Raffinate (%)
Purity	99.98	99.46	99.21	98.41
Recovery	99.57	100.00	99.34	99.14

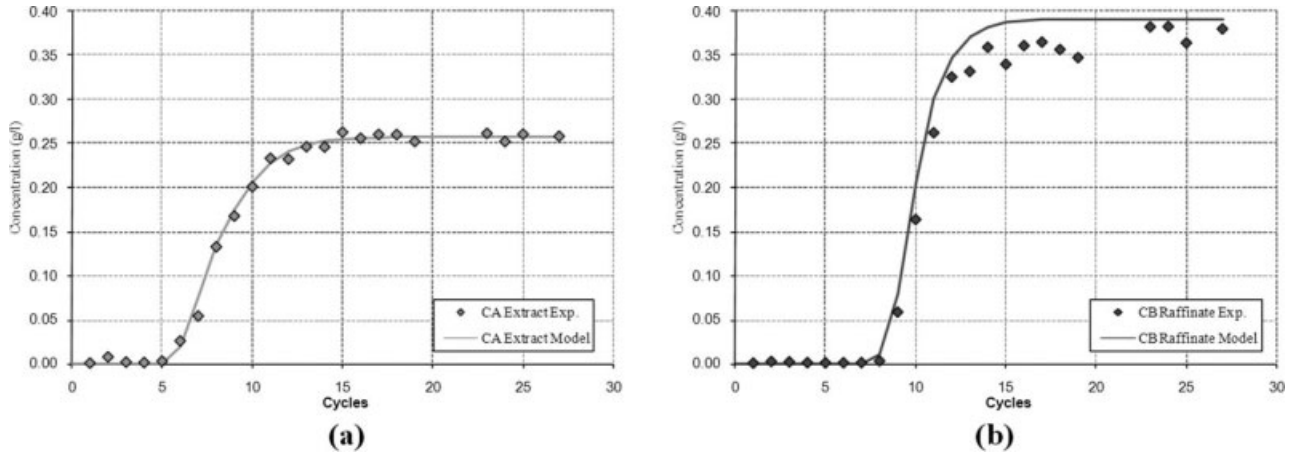

Figure 14. Experimental and simulated average concentration of (a) A in the extract and (b) B in the raffinate streams.

$Q_{II}^{*} = 36.25$ ml/min and $Q_{III}^{*} = 37.25$ ml/min, and therefore, the feed flow rate is 1.0 ml/min.

Operation and Demonstration

All SMB experiments reported in this manuscript were performed in a lab-scale unit, the FlexSMB-LSRE®, recently assembled at LSRE. The FlexSMB-LSRE® unit was operated with six preparative stainless steel columns (100 mm × 20 mm I.D. purchased from Grom Analytik HPLC GmbH, Germany (now W. R. Grace, IL) which were connected in series and packed with Chiralpak AD. For each column, a slurry of 18.5 g of Chiralpak AD (particle size 20 μm) adsorbent in 36 ml of 2-propanol was prepared in order to achieve the desired bed length. Afterwards, the columns were slowly filled with the prepared packing material and closed. The bed was compressed with pressurizing solvent (*n*-hexane/2-propanol, 90/10) at flow rate of 2 cm^3/min and pressure 30 bars at outlet of a column using an Analytical Slurry Packer from Alltech Associates.

As mentioned before, the main attribute of the described FlexSMB-LSRE® unit is a flexible valves/pumps scheme consisting of 6 SD valves and one two way valve per column (VICI AG International, Switzerland). The function of the valves is to open and close at regular time intervals and thus switch the position of inlet and outlet streams. The unit contains four HPLC pumps with a flow rate range from 0.1 to 50.0 ml/min) supplied by VWR International, LLC. To maintain a proper recycling flow rate, two Coriolis flow meters (Bronkhorst High-Tech B.V., Netherlands) are installed in the extract and raffinate lines. Moreover, two channels degasser (Flom, Japan) are installed at the feed and eluent inlet.

The operating conditions chosen before were set on the FlexSMB-LSRE® control and automation routine, written in LabView platform (National Instruments). The extract and raffinate flow rates were monitored by means of the total recovered mass in each outlet over complete cycles and weighted on a balance with 0.01 g of precision. The extract flow rate was also measured by means a Coriolis flow meter, installed for control purposes at the extract stream outlet. The recycle flow rate was monitored by the other Coriolis flow meter. The experimental average flow rates, as well as geometric features, number of columns and SMB configuration are reported in Table 4.

The internal concentration profiles at the Cyclic Steady State (CSS) were determined using the 6-port valve, which allows withdrawing the sample from the system except the

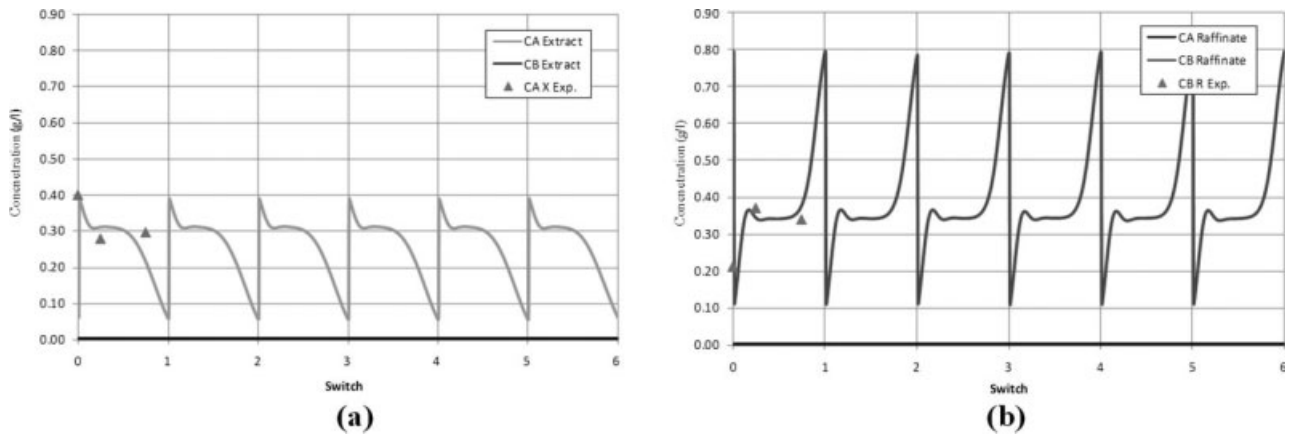

Figure 15. (a) Extract and (b) Raffinate concentration profiles over a complete cycle, during the 27th cycle.

samples of extract and raffinate, which were directly collected. Samples were taken at half of the switching time, as well as at one quarter and three quarters of the switching time.

The experimental internal concentration profile, as well as the simulation results (obtained with the detailed model) at the 27th cycle (CSS) are shown in Figure 13.

The purity and recovery of the extract and raffinate streams were calculated based on the sample collected during the whole one cycle ($6t^*$). The experimental, as well as simulated (obtained by means of the detailed model) purities and recoveries are reported in Table 5.

The experimental and simulated average concentrations in the extract and raffinate stream over 27 cycles are shown in Figure 14 and over a complete cycle during the 27th cycle are shown in Figure 15.

The experimental and simulated results are in reasonable good agreement proving that the dead volumes switching time compensating work either for the dead volumes compensating as the switching time asymmetries, providing a good separation (>98%) purity with a productivity value of 23 $g_{enantiomer}/(dm^3$ CSP day).

To better state the dead volumes methodology, one could continue to run several more experimental separations within the separation region and then plot a true, experimental, separation region, as presented in other works.[50,51]

Conclusion

When operating real SMB units several deviations are noted, when compared with the theoretical SMB apparatus. These factors should be analyzed, and if possible, minimized before the design and construction of new SMB units. An extended model, which considers different unit design particularities, can play a relevant role in the study and analysis of these operative deviations. By applying this type of model to two different units, a lab-scale (FlexSMB-LSRE®) and a pilot-scale (Licosep 12-26), it was possible to compare two different dead volumes compensating strategies and converged into only one that will easily compensate either dead volumes switching time asymmetries or delay.

By following a classical SMB separation methodology: (1) Search for the suitable stationary and mobile phases; (2) Determination of sorption parameters and their validation; (3) Modeling and design of the SMB unit; and (4) Operation and demonstration, and applying the proposed compensation measure, it was possible to separate a racemic mixture of guaifenesin with a product purities higher than 98% and to attain productivity of 23 $g_{enantiomer}/(dm^3$ CSP. day) in the FlexSMB-LSRE® unit.

Acknowledgments

Miriam Zabkova (SFRH/BPD/34828/2007, post doc grant) and Pedro Sá Gomes (SFRH/BD/22103/2005 PhD grant) gratefully acknowledge the support from "Fundação para a Ciência e Tecnologia," Ministry of Science, Technology and Higher Education of Portugal. Pedro Sá Gomes also acknowledges the Gulbenkian Foundation for supporting the presentation of part of this work at the 100th AIChE Annual Meeting, Philadelphia, PA-USA; paper 444d, "Modeling and Design Strategies for Lab-Scale SMB Units Accounting for Dead Volumes and Tubing Connections—the FlexSMB-LSRE® Unit."

Notation

A_c = cross section area, m^2
b = adsorption equilibrium constant, m^3/kg
C = bulk liquid phase concentration, kg/m^3
C_0 = initial (feed) concentration, kg/m^3
d = diameter, m
D_{ax} = axial dispersion, m^2/s
D_L = axial dispersion coefficient in packed bed, m^2/s
D_m = molecular diffusivity, m^2/s
k_{int} = internal mass transfer coefficient, m/s
L = length, m
M = molar mass of the solute, g/mol
$\langle n \rangle$ = total average solid concentration, kg/m^3
q = equilibrium adsorbed concentration, kg/m^3_{solid}
q_m = adsorbed phase saturation concentration of component, kg/m^3_{solid}
Q = liquid flow rate, m^3/s
Q_s = solid flow rate, m^3/s
r_p = particle radius, m
Re = Reynolds number
Sc = Schmidt number
Sh = Sherwood number
T = temperature, K
t = time variable, s
t^* = switching time, s
u_s = solid velocity, m/s
v = interstitial velocity, m/s
V = volume, m^3
V_m = molar volume of the adsorbate at its normal boiling temperature, m^3/mol
z = axial variable, m

Greek letters

ε = external porosity
ε_p = internal porosity
ε_T = total porosity
γ_j = ratio of fluid and solid velocity in section j
ϕ = association factor
η = viscosity, Pa s
ρ = fluid density, kg/m^3
τ = tortuosity

Subscripts and superscripts

i = species in binary mixture
j = number of section ($j = 1, 2, 3, 4$)
k = number of column ($k = 1, 2, \ldots, 6$)
c = column
tb = tube
p = particle
$*$ = operating conditions in SMB
E, F, R, X = eluent, feed, raffinate, extract SMB stream

Literature Cited

1. Okamoto Y, Ikai T. Chiral HPLC for efficient resolution of enantiomers. *Chem Soc Rev*. 2008;37:2593–2608.
2. Maier NM, Franco P, Lindner W. Separation of enantiomers: needs, challenges, perspectives. *J Chromatogr A*. 2001;906:3–33.
3. Francotte ER. Enantioselective chromatography as a powerful alternative for the preparation of drug enantiomers. *J Chromatogr A*. 2001;906:379–397.
4. Gembicki SA, Rekoske J, Oroskar AR, Johnson JA. Adsorption, liquid separation. In: Ruthven DM, editor. *Kirk-Othmer's Encyclopedia of Separation Technology*. New York: Wiley, 2002:664–691.
5. Broughton DB, Gerhold CG. *Continuous Sorption Process Employing Fixed Bed of Sorbent and Moving Inlets and Outlets*. U.S. Pat. 2,985,589, 1961.
6. Sá Gomes P, Minceva M, Rodrigues AE. Simulated moving bed technology: old and new. *Adsorption*. 2006;12:375–392.

7. Broughton DB, Neuzil RW, Pharis JM, Brearley CS. The parex process for recovering paraxylene. *Chem Eng Prog*. 1970;66:70–75.
8. Francotte ER, Richert P. Applications of simulated moving-bed chromatography to the separation of the enantiomers of chiral drugs. *J Chromatogr A*. 1997;769:101–107.
9. Juza M, Mazzotti M, Morbidelli M. Simulated moving-bed chromatography and its application to chirotechnology. *Trends Biotechnol*. 2000;18:108–118.
10. Pais LS, Loureiro JM, Rodrigues AE. Modeling, simulation and operation of a simulated moving bed for continuous chromatographic separation of 1,1′-bi-2-naphtol enantiomers. *J Chromatogr A*. 1997;827:215–233.
11. Nicoud RM, Fuchs G, Adam P, Bailly M, Kusters E, Antia FD, Reuille R, Schmid E. Preparative scale enantioseparation of a chiral epoxide: comparison of liquid chromatography and simulated moving bed adsorption technology. *Chirality*. 1993;5:267–271.
12. Cavoy E, Deltent MF, Lehoucq S, Miggiano D. Laboratory-developed simulated moving bed for chiral drug separations. *J Chromatogr A*. 1997;769:49–57.
13. Seidel-Morgenstern A, Keßler LC, Kaspereit M. New developments in simulated moving bed chromatography. *Chem Eng Technol*. 2008;31:826–837.
14. Santos MAG, Veredas V, Silva IJ Jr, Correia CRD, Furlan LT, Santana CC. Simulated moving-bed adsorption for separation of racemic mixtures. *Braz J Chem Eng*. 2004;21:127–136.
15. Pynnonen B. Simulated moving bed processing: escape from the high-cost box. *J Chromatogr A*. 1998;827:143–160.
16. Rajendran A, Paredes G, Mazzotti M. Simulated moving bed chromatography for the separation of enantiomers. *J Chromatogr A*. 2009;1216:709–738.
17. Miller L, Grill C, Yan T, Dapremont O, Huthmann E, Juza M. Batch and simulated moving bed chromatographic resolution of a pharmaceutical racemate. *J Chromatogr A*. 2003;1006:267–280.
18. Wu DJ, Xie Y, Ma Z, Wang N-HL. Design of simulated moving bed chromatography for amino acid separations. *Ind Eng Chem Res*. 1998;37:4023–4035.
19. Xie Y, Mun S, Kim J, Wang N-HL. Standing wave design and experimental validation of a tandem simulated moving bed process for insulin purification. *Biotechnol Prog*. 2002;18:1332–1344.
20. Sá Gomes P, Zabka M, Zabkova M, Minceva M, Rodrigues AE. *Separation of Fine Chemical Species by Means of Continuous Chromatography: the Simulated Moving Bed Technology*, In AIChE Annual Meeting, Philadelphia, PA, USA, 2008.
21. Negawa M, Shoji F. Optical resolution by simulated moving-bed adsorption technology. *J Chromatogr*. 1992;590:113–117.
22. Abel S, Juza M. Less common applications of enantioselective HPLC using the SMB technology in the pharmaceutical industry. In: Subramanian G, Editor. *Chiral Separation Techniques*, 3rd ed. Weinheim, Germany: Wiley-VCH Verlag GmbH & Co., 2007:203–273.
23. Ludemann-Hombourger O, Nicoud RM, Bailly M. The 'VARICOL' process: a new multicolumn continuous chromatographic process. *Sep Sci Technol*. 2000;35:1829–1862.
24. Zhang Z, Mazzotti M, Morbidelli M. PowerFeed operation of simulated moving bed units: changing flow-rates during the switching interval. *J Chromatogr A*. 2003;1006:87–99.
25. Zang Y, Wankat PC. SMB operation strategy—partial feed. *Ind Eng Chem Res*. 2002;41:2504–2511.
26. Schramm H, Kaspereit M, Kienle A, Seidel-Morgenstern A. Simulated moving bed process with cyclic modulation of the feed concentration. *J Chromatogr A*. 2003;1006:77–86.
27. Schramm H, Kaspereit M, Kienle A, Seidel-Morgenstern A. Improving simulated moving bed processes by cyclic modulation of the feed concentration. *Chem Eng Technol*. 2002;25:1151–1155.
28. Sá Gomes P, Rodrigues AE. Outlet streams swing (OSS) and Multi-Feed operation of simulated moving beds. *Sep Sci Technol*. 2007;42:223–252.
29. Abdelmoumen S, Muhr L, Bailly M, Ludemann-Hombourger O. The M3C process: a new multicolumn chromatographic process integrating a concentration step. I—the equilibrium model. *Sep Sci Technol*. 2006;41:2639–2663.
30. Bailly M, Nicoud R-M, Adam P, Ludemann-Hombourger O. *Method and Device for Chromatography Comprising a Concentration Step*. EP 20,030,767,859, 2005.
31. Paredes G, Rhee HK, Mazzotti M. Design of simulated-moving-bed chromatography with Enriched Extract operation (EE-SMB): Langmuir isotherms. *Ind Eng Chem Res*. 2006;45:6289–6301.
32. Minceva M, Rodrigues AE. Influence of the transfer line dead volume on the performance of an industrial scale simulated moving bed for p-xylene separation. *Sep Sci Technol*. 2003;38:1463–1497.
33. Blehaut J, Nicoud RM. Recent aspects in simulated moving bed. *Analusis*. 1998;26:M60–M70.
34. Hotier G, Nicoud R-M. *Chromatographic Simulated Mobile Bed Separation Process with Dead Volume Correction Using Period Desynchronization*. U.S. Pat. 5,578,215, 1996.
35. Migliorini C, Mazzotti M, Morbidelli M. Simulated moving-bed units with extra-column dead volume. *AIChE J*. 1999;45:1411–1420.
36. Mun S, Xie Y, Wang NHL. Robust pinched-wave design of a size-exclusion simulated moving-bed process for insulin purification. *Ind Eng Chem Res*. 2003;42:3129–3143.
37. Gonçalves CV, Carpes MJS, Correia CRD, Santana CC. Purification of n-boc-Rolipram racemate on chiral stationary phase using simulated moving bed chromatography under linear conditions. *Biochem Eng J*. 2008;40:526–536.
38. Zabka M, Minceva M, Sá Gomes P, Rodrigues AE. Chiral separation of R,S-a- tetralol by simulated moving bed. *Sep Sci Technol*. 2008;43:727–765.
39. Blehaut J, Charton F, Nicoud R-M. Separation of fatty alcohol stereoisomers on a large-scale high-performance simulated moving bed, In LC-GC International, 1996:228–238.
40. Zabka M, Rodrigues AE. Thermodynamic and kinetic study of adsorption of R,S-?-Tetralol enantiomers on the chiral adsorbent CHIRALPAK AD. *Sep Sci Technol*. 2007;42:739–768.
41. Pais LS, Loureiro JM, Rodrigues AE. Modeling strategies for enantiomers separation by SMB chromatography. *AIChE J*. 1998;44:561–569.
42. Storti G, Mazzotti M, Morbidelli M, Carra S. Robust design of binary countercurrent adsorption separation processes. *AIChE J*. 1993;39:471–492.
43. Mazzotti M, Storti G, Morbidelli M. Optimal operation of simulated moving bed units for nonlinear chromatographic separations. *J Chromatogr A*. 1997;769:3–24.
44. Azevedo DCS, Rodrigues AE. Design of a simulated moving bed in the presence of mass-transfer resistances. *AIChE J*. 1999;45:956–966.
45. Mun S, Wang NHL, Koo YM, Yi SC. Pinched wave design of a four-zone simulated moving bed for linear adsorption systems with significant mass-transfer effects. *Ind Eng Chem Res*. 2006;45:7241–7250.
46. Imamoglu S. Simulated moving bed chromatography (SMB) for application in bioseparation. *Adv Biochem Eng/Biotechnol*. 2002;76:211–231.
47. Hotier G, Nicoud R-M. Separation process by simulated moving bed chromatography with correction for dead volume by desynchronisation of periods. EP 0,688,589, 1995.
48. Katsuo S, Langel C, Schanen P, Mazzotti M. Extra-column dead volume in simulated moving bed separations: theory and experiments. *J Chromatogr A*. In Press.
49. Mun S, Xie Y, Kim JH, Wang NHL. Optimal design of a size-exclusion tandem simulated moving bed for insulin purification. *Ind Eng Chem Res*. 2003;42:1977–1993.
50. Mihlbachler K, Fricke J, Yun T, Seidel-Morgenstern A, Schmidt-Traub H, Guiochon G. Effect of the homogeneity of the column set on the performance of a simulated moving bed unit. I. Theory. *J Chromatogr A*. 2001;908:49–70.
51. Mihlbachler K, Jupke A, Seidel-Morgenstern A, Schmidt-Traub H, Guiochon G. Effect of the homogeneity of the column set on the performance of a simulated moving bed unit. II. Experimental study. *J Chromatogr A*. 2002;944:3–22.
52. Glueckauf E. Theory of chromatography. Part 10 formulae for diffusion into spheres and their application to chromatography. *Trans Faraday Soc*. 1955;51:1540–1551.
53. Reid RC, Prausnitz JM, Poling BE. *Properties of Gas and Liquids*, 4th ed. New York: McGraw Hill, 1987.
54. Pais LMS. Chiral separation by simulated moving bed chromatography, PhD Thesis, University of Porto, Portugal, 1999.

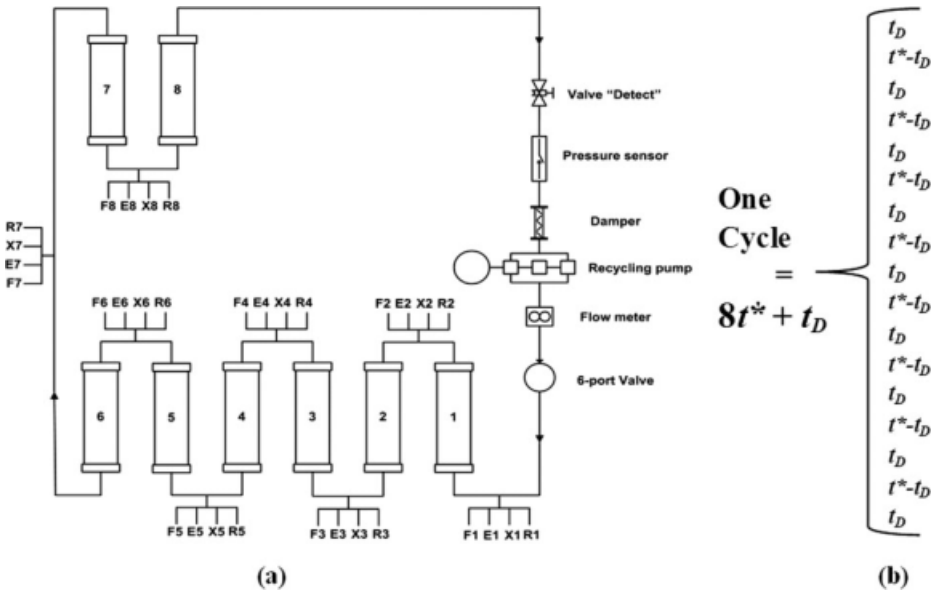

Figure B1. (a) Licosep 12-26 SMB unit scheme and (b) recycle pump compensating strategy for a eight columns configuration.

Appendix A

The fixed bed model used for the simulation of the frontal analysis experiments is established by performing a mass balance to species i (A: S-guaifenesin and B: R-guaifenesin) in the bulk liquid phase (Eq. A1) and in the adsorbent particle (Eq. A2):

$$\varepsilon \frac{\partial C_i}{\partial t} = \varepsilon D_{\mathrm{L}} \frac{\partial^2 C_i}{\partial z^2} - \varepsilon v \frac{\partial C_i}{\partial z} - (1-\varepsilon)\frac{3}{r_{\mathrm{p}}} k_{\mathrm{int}_i}(C_i - C_{\mathrm{p}_i}) \quad \text{(A1)}$$

$$\varepsilon_{\mathrm{p}} \frac{\partial C_{\mathrm{pi}}}{\partial t} + (1-\varepsilon_{\mathrm{p}})\frac{\partial q_i}{\partial t} = \frac{3}{r_{\mathrm{p}}} k_{\mathrm{int}_i}(C_i - C_{\mathrm{pi}}) \quad \text{(A2)}$$

With the multicomponent adsorption equilibrium isotherm: $q_i = f(C_{\mathrm{p}_i})$, in this case presented before by Eq. 2.

The initial conditions:

$$t = 0: \; C_i = C_{\mathrm{pi}} = q_i = 0 \quad \text{(A3)}$$

The Danckwerts boundary conditions at the column inlet ($z = 0$) and column exit ($z = L$) for ($t > 0$) as follows:

$$z = 0: \; D_{\mathrm{L}} \frac{\partial C_i}{\partial z} = v_z (C_i - C_i^{\mathrm{in}}) \quad \text{(A4a)}$$

$$z = L: \; \frac{\partial C_i}{\partial z} = 0 \quad \text{(A4b)}$$

With C_i, representing the concentration in the bulk fluid; C_{p_i}, the average concentration in the particle pores; q_i, the adsorbed

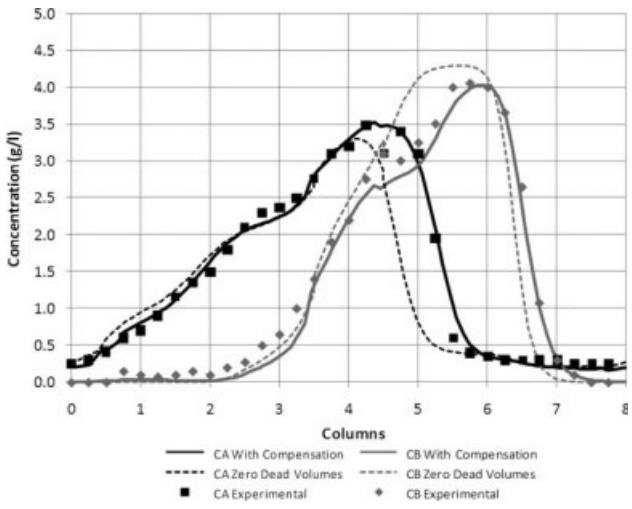

Figure B2. Concentration profiles, experimental and simulated with model presented before (Zero Dead Volumes) and considering both the unit's dead volumes as compensating measure (with compensation).

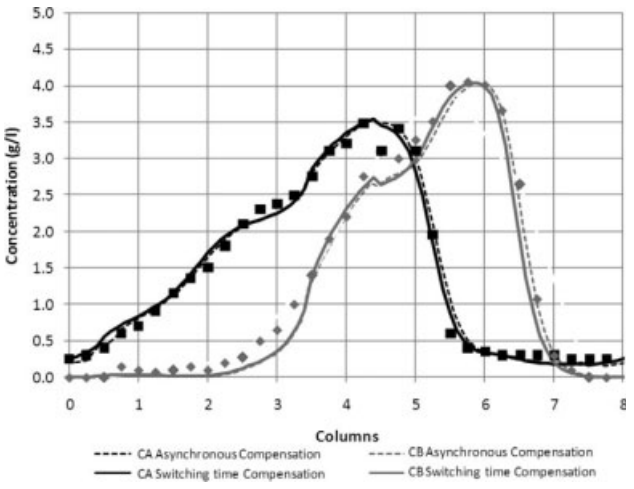

Figure B3. Concentration profiles, experimental and simulated using the asynchronous and switching time compensation strategies.

Table B1. Purity Values for Experimental and Simulate by Mean of the Detailed Model, Accounting for Unit's Dead Volumes and Recycle Pump Dead Volumes Compensation

Purity	Experimental (%)	Comp. Simulated (%)
A Extract	90.00	96.95
B Raffinate	91.60	89.08

phase concentration in equilibrium with C_{p_i}; v_z, the interstitial velocity; D_L, the axial dispersion coefficient; ε, ε_p the bed and particle porosity, respectively; k_{inti}, the internal mass transfer coefficient and r_p, the radius of the adsorbent particle.

The mass transfer was calculated as mentioned using an approximation suggested by Glueckauf[52] given by $k_{inti} = \frac{5\varepsilon_p D_m}{\tau r_p}$ where, D_m is the free molecular diffusivity and τ is the tortuosity factor, estimated by $\tau = \frac{(2-\varepsilon_p)^2}{\varepsilon_p}$. The molecular diffusivity of the solute guaifenesin enantiomers was calculated by the Wilke-Chang equation extended to mixed solvents by Perkins and Geankoplis $D_m = 7.4 \times 10^{-8} \frac{T\sqrt{\phi M_i}}{\eta V_{mi}^{0.6}}$ where T (K) is the absolute temperature, η (cP) is the mobile phase viscosity, calculated according to Teja and Rice method for liquid mixture. The molar volume of the adsorbate at its normal boiling temperature V_m (cm^3/mol) was estimated by the Le Bas method.[53] The molecular diffusivity of each enantiomer is similar and therefore the internal mass transfer coefficient k_{inti} is identical for both enantiomers.

Appendix B

As mentioned before, each SMB unit design has its own particularities that will probably lead to discrepancies between the experimental results and the ones simulated by the most common models. Nevertheless, one can also extend these models by introducing the specific units' design particularities.

This methodology was applied in modelling of the Licosep 12-26 unit before,[38] where the tubing and equipment dead volumes were introduced in the SMB model and describe by means of an axial dispersive plug flow in a tube, as follows,

$$\frac{\partial C_{itb}}{\partial t} = D_{axtb}\frac{\partial^2 C_{itb}}{\partial z^2} - v_{tb}\frac{\partial C_{itb}}{\partial z} \tag{B1}$$

where the D_{axtb} represents the axial dispersion coefficient calculated for a tube of 1 mm i.d., C_{itb} the species i concentration in tube tb and v_{tb} the velocity in tube tb.

As noted before, the Licosep unit implements a compensation measure to avoid asymmetries due to the dead volume introduced by the recycle pump (Figure B1a). Namely, all valves passing the recycle pump are shifted with a delay of $t_D = \frac{V_{Li}^D}{\bar{Q}_j^*}$, as represented in Figure B1b, for the case of 8 columns SMB unit.

This model was applied for the simulation of an SMB chiral epoxide enantiomers separation with microcrystalline cellulose triacetate,[54] characterized by the following multicomponent equilibrium isotherms:

Table B2. Purity Values for Simulate Results Obtained by the Two Different Compensation Strategies: Asynchronous and Switching time

Purity	Switching Time (%)	Asynchronous (%)
A Extract	97.08	96.95
B Raffinate	89.61	89.08

$$q_A = 1.35C_{pA} + \frac{7.32 \times 0.163C_{pA}}{1 + 0.163C_{pA} + 0.087C_{pB}} \tag{B2}$$

$$q_B = 1.35C_{pB} + \frac{7.32 \times 0.087C_{pB}}{1 + 0.163C_{pA} + 0.087C_{pB}} \tag{B3}$$

In a unit configuration of two columns per section, and that run with a t_D 25% higher than should be need (it would easy to model a unit that is compensating well the dead volumes, but it is quite more difficult to do it with one unit that is compensating more, less than it should), and by these means testing both the dead volumes as well as the compensating strategy procedure, resulting in the following concentration profiles, Figure B2,

The comparison of the experimental and calculated SMB performance parameters using the detailed model, accounting for the unit's dead volumes and recycle pump dead volumes compensation is given in Table B1.

As can be noted from Figure B2 and Table B1 the model gives reasonable prediction of the experimental data.

From the scheme in Figure B1b, it is possible to note that the asynchronous shifting measure used to compensate the recycle pump dead volume, results in a global switching time increase, over a complete cyclic. By simulating now the Licosep SMB unit running without compensation (still with the same dead volumes as presented before), with the same operating parameters but with corrected switching time:

$$t^*|_{Licosep} = t^*|_{SMB} + \frac{V_{Li}^D}{\bar{Q}_j^*}\frac{1}{\sum_{j=1}^{IV} Nc_j} \tag{B7}$$

The experimental and calculated SMB concentration profiles using the asynchronous and switching time compensation strategy are presented in Figure B3.

The product purity values obtained by the Asynchronous and Switching time compensation strategy are presented in Table B2.

As can be observed from Figure B2 and Table B2, the two strategies converged to the same, and therefore we will use the switching time compensating strategy, avoiding several problems related with the hereby-called asynchronous compensating strategy.

Manuscript received Jan. 13, 2009, and revision received Apr. 29, 2009.